Evidence of magma-water interaction during the 13,800 years BP explosive cycle of the Licán Ignimbrite, Villarrica volcano (southern Chile)

Silke Lohmar
Departamento de Geología, Universidad de Chile, Plaza Ercilla 803, Santiago, Chile
Université Blaise Pascal, Observatoire de Physique du Globe, Laboratoire CNRS Magmas et Volcans, 5 rue Kessler, 63038 Clermont-Ferrand, France
slohmar@cec.uchile.cl

Claude Robin
Departamento de Geología, Universidad de Chile, Plaza Ercilla 803, Santiago, Chile
IRD, Unité Mixte 163, Laboratoire CNRS Magmas et Volcans, 5 rue Kessler, 63038 Clermont-Ferrand, France
Claude. Robin@ird.fr

Alain Gourgaud
Université Blaise Pascal, Observatoire de Physique du Globe, Laboratoire CNRS Magmas et Volcans, 5 rue Kessler, 63038, Clermont-Ferrand, France
A.Gourgaud@opgc.univ-bpclermont.fr

Jorge Clavero
Servicio Nacional de Geología y Minería, Avenida Santa María 0104, Santiago, Chile
jclavero@sernageomin.cl

Miguel Ángel Parada
Departamento de Geología, Universidad de Chile, Plaza Ercilla 803, Santiago, Chile
maparada@cec.uchile.cl

Hugo Moreno
Observatorio Volcanológico de los Andes del Sur, Servicio Nacional de Geología y Minería, Cerro Ñielol s/n, Casilla 23-D, Temuco, Chile
hmoreno@sernageomin.cl

Orkun Ersoy
Hacettepe University, Department of Geological Engineering, 06532 Beytepe, Ankara, Turkey
Université Blaise Pascal, Observatoire de Physique du Globe, Laboratoire CNRS Magmas et Volcans, 5 rue Kessler, 63038 Clermont-Ferrand, France
oersoy@hacettepe.edu.tr

Leopoldo López-Escobar
Instituto de Geología Económica Aplicada, Universidad de Concepción, Casilla 160-C, Concepción, Chile
llopez@udec.cl

José Antonio Naranjo
Servicio Nacional de Geología y Minería, Avenida Santa María 0104, Santiago, Chile
jnaranjo@sernageomin.cl

ABSTRACT

Villarrica is an active stratovolcano located in the Southern Andean Volcanic Zone. About 13,800 years BP (conventional radiocarbon ages), this volcano experienced major explosive eruptions which resulted in the emission of a sequence of pyroclastic flows, known as the 'Licán Ignimbrite', the bulk volume of which is estimated in ~10 km^3 (non-DRE, Dense Rock Equivalent). The deposits mainly consist of massive pyroclastic flows and stratified pyroclastic surges. Typical flow facies show scoriaceous bombs, dense juvenile blocks, lithics and scoria lapilli immersed in a dark-grey to brownish matrix, whereas surges expose lapilli-sized scoria in a fine, light-brown or yellow-green matrix. Juvenile clasts range from 55 to 58 wt% SiO_2 in composition. This paper describes the general architecture of the Licán Ignimbrite deposits and, based on SEM (Scanning Electron Microscope) observations and lithologic data, emphasizes the role of fragmentation due to magma-water interaction during the eruption. The results indicate that gas expansion was an important process. However, field characteristics, surface textures of ashes, enrichment of lithics towards the top of the sequence and variable palagonitization of matrix glass show the intervention of water since the initial stages of the eruption and its increasing influence during the later phases.

Key words: Explosive volcanism, Mafic pyroclastic flows, Phreatomagmatism, Southern Andean Volcanic Zone, Villarrica volcano, Chile.

Revista Geológica de Chile, Vol. 34, No. 2, p. 233-247, 9 Figs., 2 tables, July 2007.

RESUMEN

Evidencias de interacción magma-agua durante el ciclo eruptivo explosivo de la Ignimbrita Licán (13.800 años AP), volcán Villarrica (sur de Chile). El Villarrica es un estratovolcán activo, situado en la Zona Volcánica de los Andes del Sur. Hace aproximadamente 13.800 años AP (edades ^{14}C no calibradas), este volcán sufrió un evento explosivo importante que dio lugar a la emisión de una secuencia de flujos piroclásticos, conocida como la 'Ignimbrita Licán', cuyo volumen ha sido estimado en ~10 km^3 (no-ERD, Equivalente de Roca Densa). Los depósitos consisten, principalmente, en flujos piroclásticos macizos y oleadas piroclásticas estratificadas. Las facies típicas que resultan de los flujos presentan bombas escoriáceas, bloques juveniles densos, fragmentos líticos y lapilli escoriáceo, inmersos en una matriz cuyo color varía entre gris oscuro y pardo. Por otro lado, los depósitos de oleadas están constituidos por escorias de tamaño lapilli, contenidas en una matriz fina, de color pardo claro o amarillo verdusco. La composición de los clastos juveniles es andesítico-basáltica a andesítica (55 a 58% en peso de SiO_2). Este artículo presenta la estructura interna general de estos depósitos, observaciones realizadas en el MEB (Microscopio Electrónico de Barrido) y datos litológicos y granulométricos, con el propósito de determinar el papel que jugó la fragmentación debido a la interacción magma-agua durante la erupción. Los resultados indican que la expansión de gases pudo ser un proceso importante. Sin embargo, características de terreno, texturas superficiales de cenizas, el enriquecimiento en fragmentos líticos hacia el techo de las secuencias y la palagonitización variable del vidrio de la matriz sugieren un incremento de la intervención del agua durante el transcurso de la erupción.

Palabras claves: Volcanismo explosivo, Flujos piroclásticos máficos, Freatomagmatismo, Zona Volcánica de los Andes del Sur, Volcán Villarrica, Chile.

INTRODUCTION

Villarrica volcano, located at 39°25'S, 71°57'W and 2,847 m a.s.l. (Fig. 1), is currently the most active volcano of the Southern Andean Volcanic Zone (Petit-Breuilh and Lobato, 1994; González-Ferrán, 1995). It is located at the western end of a N50-60°W volcanic alignment formed by Villarrica, Quetrupillán and Lanín volcanoes (López-Escobar *et al.*, 1995; Lara, 2004; Fig. 2). This alignment is oblique to the major structural feature of the Southern Andean region, the NNE trending Liquiñe-Ofqui Fault Zone, which extends over 1,000 km between latitudes 38° and 47°S (Cembrano *et al.*, 1996; Fig. 1). The Villarrica edifice has a volume of about 250 km^3 and its products cover more than 700 km^2 of the surrounding area (Moreno, 1993)[1]. The volcano lies on a basement comprising volcanic, volcaniclastic and plutonic rocks, and scarce metamorphic and sedimentary rocks of Palaeozoic to Pliocene age (Moreno and Clavero, 2006).

Since the end of the last glaciation (~ 14 ka, see Regional Late Glacial History, next page), eruptive activity at Villarrica includes mainly basalts and basaltic andesite lava flows and pyroclastic deposits. About thirty parasitic cones, the majority of which are basic to intermediate in composition and of Holocene age, are located on the flanks of the volcano. In spite of being an overall mafic composition, generally characterised by effusive or slightly explosive volcanism, Villarrica has generated several large explosive eruptions. Two of these, the Licán and Pucón ignimbrites, produced large-volume pyroclastic flow deposits (Clavero and Moreno, 1994; 2004) with juvenile material of basaltic andesite to andesite compositions. In order to investigate the causes of such relatively uncommon eruptive products, a study has been undertaken in an IRD (Institut de Recherche pour le Développement, France)-GEA (Instituto de Geología Económica Aplicada, Universidad de Concepción, Chile)-SERNAGEOMIN (Servicio Nacional de Geología y Minería, Chile)-Universidad de Chile collaborative project (ECOS-CONICYT C01U03). In this paper, we present the stratigraphy and lithological characteristics of the deposits from the largest explosive eruption, which occurred in the Late Glacial Period and resulted in the Licán Ignimbrite. Lithological countings, grain-size analyses, coupled with SEM and field observations, led to a better understanding of the role of phreatomagmatism in the generation of these voluminous and relatively basic pyroclastic flow deposits.

[1] Moreno, H. 1993. Volcán Villarrica: Geología y evaluación del riesgo volcánico, regiones IX y X, 39°25'S. Informe final (Unpublished), Proyecto Fondecyt, No. 1247: 112 p.

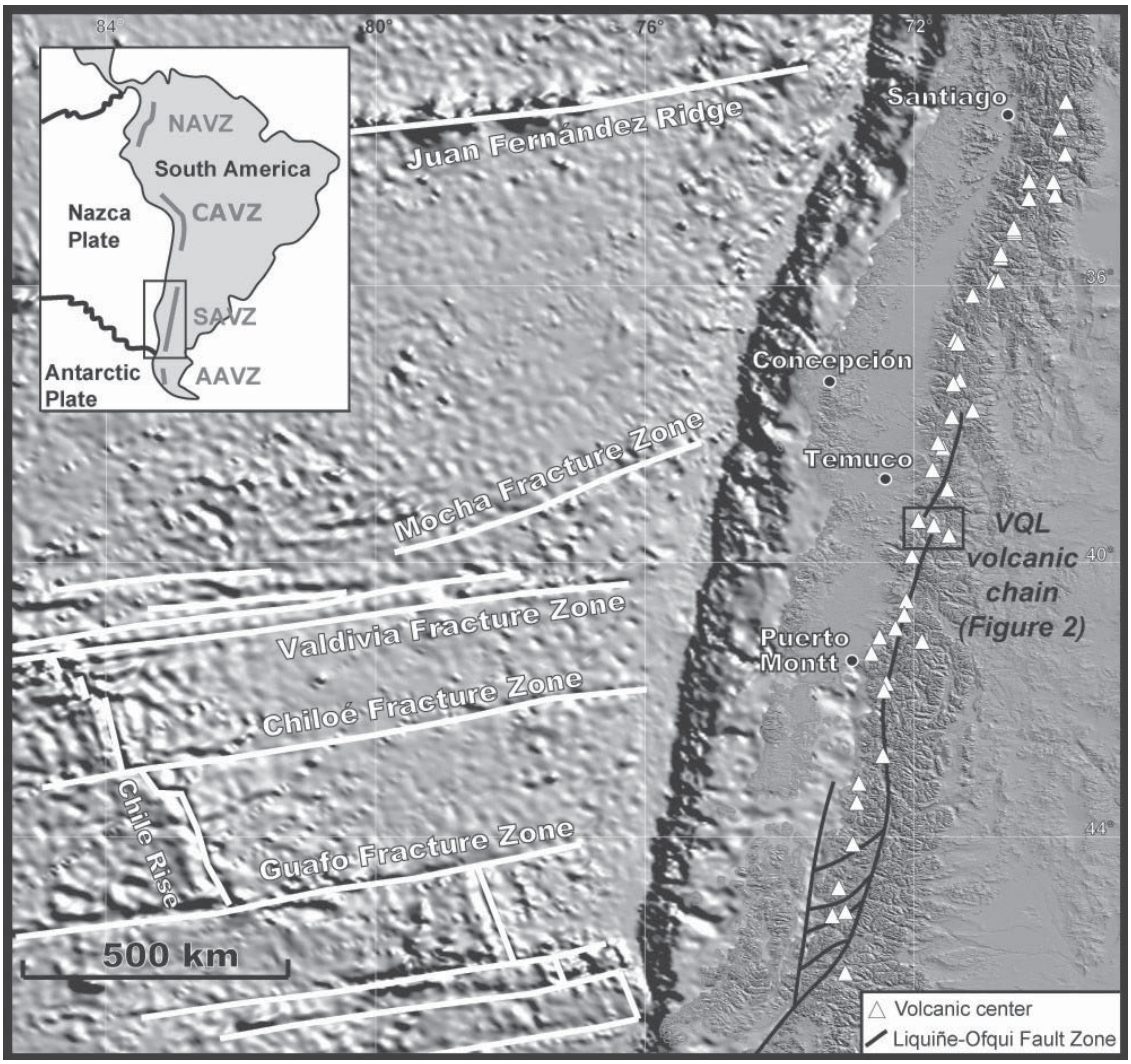

FIG. 1. Location of Villarrica, Quetrupillán and Lanín (**VQL**) volcanic chain in the Southern Andean Volcanic Zone (**SAVZ**). Detail of area of interest is shown in figure 2. Base images are shaded DEM (SRTM) and bathymetry (Etopo 2). On the left, the inset shows the position of the SAVZ relative to the Northern, Central and Austral Andean volcanic zones (**NAVZ**, **CAVZ** and **AAVZ**, respectively). Names of fracture zones on the oceanic Nazca plate are taken from Herron *et al.* (1981) while the position of the Liquiñe-Ofqui Fault Zone is taken from Cembrano *et al*. (1996).

VOLCANOLOGIC CONTEXT AND AGE OF THE LICÁN IGNIMBRITE

REGIONAL LATE GLACIAL HISTORY

Villarrica volcano is situated at the northern end of the Chilean Lake District (40-43°S). In this region, the Llanquihue glaciation (equivalent to the Würm glaciation in the Alps or the Wisconsin glaciation in North America) extended between 75 and 14 ka, approximately (Clapperton, 1993), building up extensive icefields. Denton *et al*. (1999) have identified the last glacial advance at 14,805-14,550 years BP (conventional radiocarbon ages, with present= 1950) as the last of a series of four in the last 30,000 years. The end of the last glacial period was a world-wide event (*e.g.*, Lowell *et al.*, 1995). In the

Chilean Lake District, there was a marked warming beginning at 14,600-14,300 years BP followed by either a gradual transition or a stepped increase in temperature that culminated at *ca.* 13,000-12,700 years BP (McCulloch *et al.*, 2000).

VOLCANOLOGIC CONTEXT OF THE LICÁN IGNIMBRITE

$^{40}Ar/^{39}Ar$ dating of basal volcanic rocks from Villarrica suggests a first construction phase between *ca.* 600 and 100 ka, which consisted in the emission of lava flows and volcanic breccias of laharic and pyroclastic origin, basaltic to andesitic in composition (Moreno and Clavero, 2006). Approximately 100 ka years ago, the collapse of a 6.5 x 4.2 km-wide caldera occurred (caldera 1 in Fig. 2) and was followed by the extrusion of dacitic domes (Clavero and Moreno, 2004). Volcanic activity continued probably until the generation of the Licán Ignimbrite during the Late Glacial Period.

^{14}C dating of charcoal in two pyroclastic flow deposits belonging to the Licán Ignimbrite resulted in ages of 13,990±100 and 13,910±60 years BP (conventional radiocarbon ages, corrected using ^{13}C and calculated with the Libby half-life of 5,568 years; Center for Isotope Research, Groningen, Netherlands). These ages are close to the average age of 13,800-13,850 years BP, obtained from thirteen ^{14}C datings by Moreno and Clavero (2006 and references therein) and confirms that the Licán Ignimbrite was emitted several centuries after the warming event which started 14,600 ^{14}C years BP. The Licán Ignimbrite would be related to a collapse which affected the upper part of the cone and would have rejuvenated the older caldera structure (caldera 1 in Fig. 2; Clavero and Moreno, 1994).

Subsequently, a new cone grew on the northwestern edge of the nested caldera, which was truncated by the eruption of the Pucón Ignimbrite, generating caldera 2 (Fig. 2). This eruption has been dated at 3,700 years BP (Clavero and Moreno, 1994) and has a bulk volume of ~3 km^3 (Silva *et al.*, 2004). Since four millenia, the eruptive activity, mainly effusive, has also comprised pyroclastic episodes of lower explosivity than those that generated the Licán and Pucón ignimbrites. As a whole, the emission of lava flows has dominated the activity of Villarrica volcano during the last 14 ka. Nevertheless, at least 16 pyroclastic flow/surge deposits have been recognized, including the Licán and Pucón deposits (Moreno, 1993)[1].

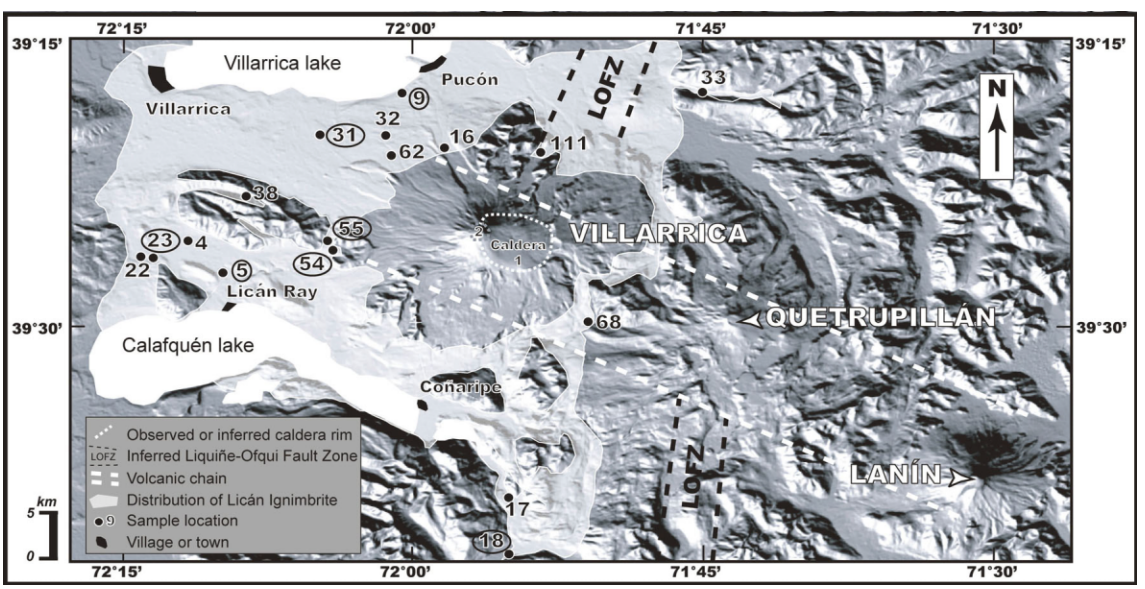

FIG. 2. DEM image showing the VQL volcanic chain and extension of the Licán Ignimbrite from Villarrica volcano (the latter according to Clavero, 1996). Sample locations, where grain size studies, lithological analyses and surface texture observations have been made, are circled.

CHARACTERISTICS OF THE LICÁN DEPOSITS

FIELD CHARACTERISTICS

The extent, volume estimation (10 km^3, non-DRE) and detailed outcrop descriptions of the Licán Ignimbrite have been given by Clavero (1996). The deposits are radially distributed around the volcanic edifice, covering an area of about 1,000 km^2 (Fig. 2). Two main facies are recognized:

Massive scoria flow deposits. To the north and northwest of the volcano, the deposits consist mainly of massive metric to decametric-thick beds of ash and scoria emplaced as pyroclastic density currents strongly controlled by the topography (Fig. 3A, B), whereas to the southwest and south, massive beds mantle the pre-existing topography. No evidence of pyroclastic flow deposits are observed at altitudes higher than 850 m a.s.l., probably due to the 'ice effect' (Clavero, 1996). The maximum thickness observed for a single bed is ~25 m on the northeast side of the volcano, in the Río Pedregoso valley at 620 m a.s.l. (site 111, Figs. 2, 3A). Scoria blocks and bombs represent 15 to 20% of the volume of the deposit; the bombs commonly show prismatic fracturing and cauliform surfaces, and commonly contain volcanic and granitoid xenoliths (Fig. 3C). The matrix, sometimes indurated, is dark-grey, brown or brown-orange in colour. Fieldwork shows composite sequences and differences in the architecture of the deposits, related to facies changes with direction and distance from the vent. For example, at the foot of the cone (~8 km from the summit), in a north westward direction (Río Correntoso valley, site 62, Fig. 2), the sequence consists of a basal fallout lapilli layer (Fig. 3D) followed by ash and scoria flow deposits with carbonized wood at their base (^{14}C age: 13,910±60 years BP). This sequence is underlain directly by an undated sequence, up to 6 m thick, of a massive agglomerate (3.5 m thick, lower part) and a fine, clay-rich and weathered ash flow deposit (2.5 m thick, upper part) (Fig. 4). These basal deposits represent either the lower unit of the observed Licán Ignimbrite or, more probably, previous explosive eruptions, as suggested by the occurrence of similar pyroclastic events during the Llanquihue glaciation (Gaytán *et al.*, 2005). To the southwest of the volcano (for example, site 5, location on Fig. 2), a characteristic log of the Licán deposits exposes at least three flow units (Fig. 4).

Cross-bedded deposits. Surge deposits have been observed in the upper part of the sequences, as at sites 5 and 23, near Licán Ray (Fig. 2). They consist of light brown to yellow-green, cross-bedded layers of ash and small lapilli, whose total thickness can reach up to several meters, although it is usually one meter or less. Abundant pieces of charcoal are present in these surge deposits widespread to the west and southwest, even on top of the hills. The transition from ash and scoria flow deposits to the surge sequence, which marks the end of the eruption, is characterised by a drastic change in colour, from dark-grey to light-brown, and by an increase in lithic contents. Due to topography effects, a basal surge is also observed in some places, as already reported by Clavero (1996).

GRAIN SIZE

Grain-size analyses were carried out on 10 samples using the phi scale between -5 and 4 (32 mm to 63 microns; Vennat, 2003)[2]. The weights were measured with a 0.001 g precision. Histograms show bimodal or even polymodal distributions (Fig. 5A). Samples from the upper parts of the sequences (including upper surge deposits) show lower mean values of grain size (higher on phi scale) than those from the lower and central horizons (Fig. 5B), indicating an enrichment in finer particles to the top of the sections. In a diagram of median diameter *versus* sorting index (not shown), the points of the analyzed samples plot mainly in the field of pyroclastic flows (Walker, 1971) and surges (Fisher and Schmincke, 1984 and references therein). The sorting index for Licán pyroclastic flow samples ranges from 1.72 to 2.79. Considering that 90% of Walker's (1971) data have sorting indices between 2.0 and 4.5, these values indicate a relatively good sorting.

[2] Vennat, J. 2003. Caractérisation physique des pyroclastites post-glaciaires du volcan Villarrica. Travail d'Etude et de Recherche (Unpublished), Université Blaise Pascal, Laboratoire Magmas et Volcans: 32 p.

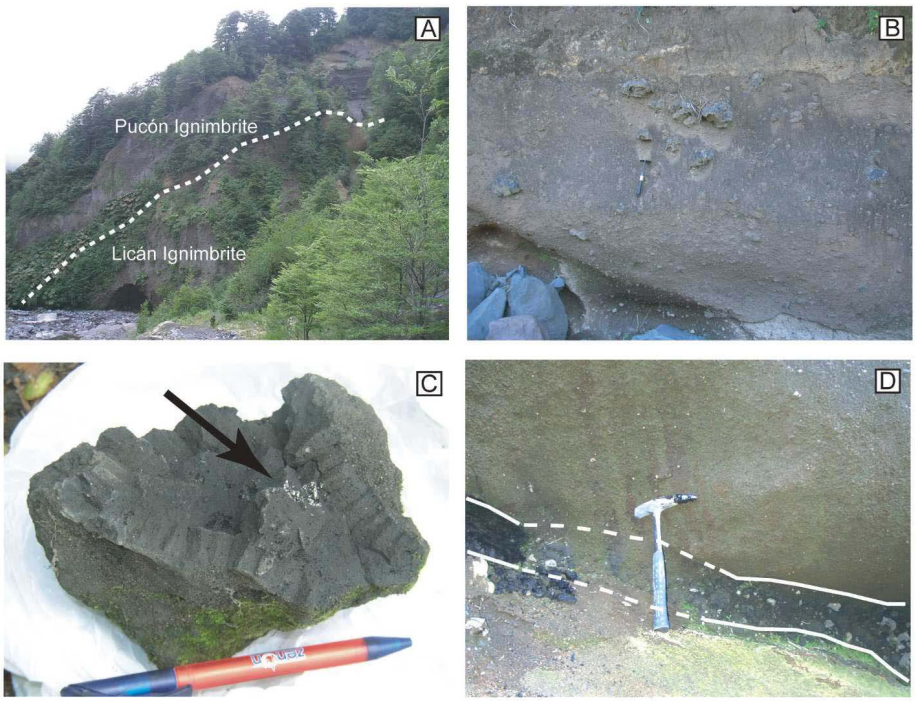

FIG. 3. Conspicuous field features of the Licán Ignimbrite.
Picture A: comes from a section to the NNE of Villarrica volcano (sample location 111, Fig. 2), showing the massive 25 m-thick Licán Ignimbrite below Pucón Ignimbrite.
Picture B: shows the detail of a massive Licán unit to the northwest of Villarrica volcano (sample site 62).
Picture C: shows typical bombs from the Licán Ignimbrite, with prismatically jointed rims and granitoid inclusions (arrow).
Picture D: exhibits the initial fallout deposit at the base of a massive ignimbrite facies at site 62.

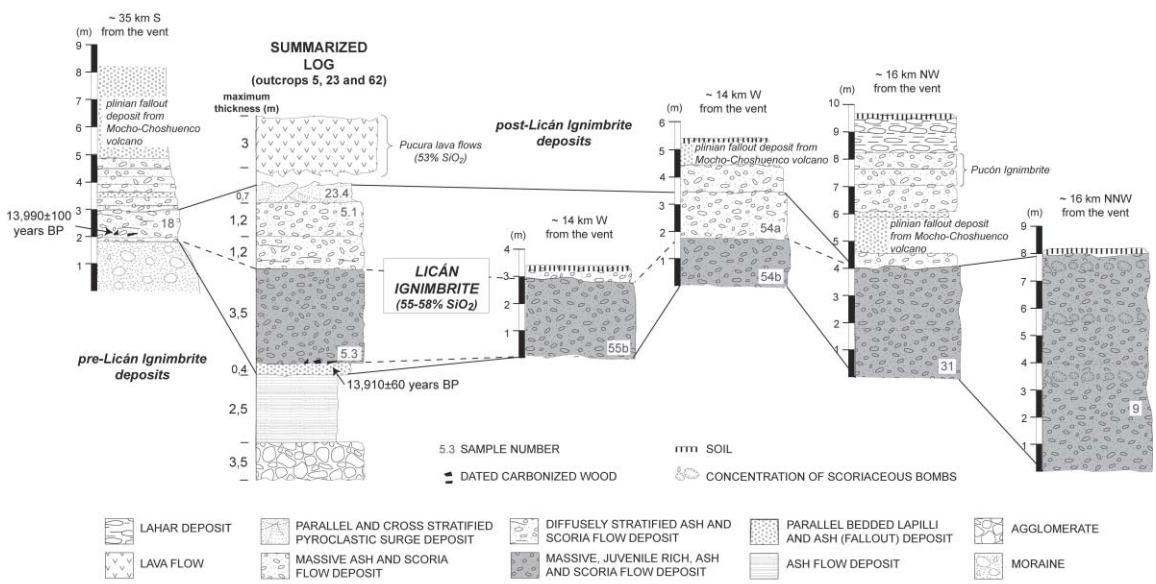

FIG. 4. Summarized log for the Licán Ignimbrite showing lithological facies, relationships with previous and further deposited units and correlation with different outcrops studied around the volcano.

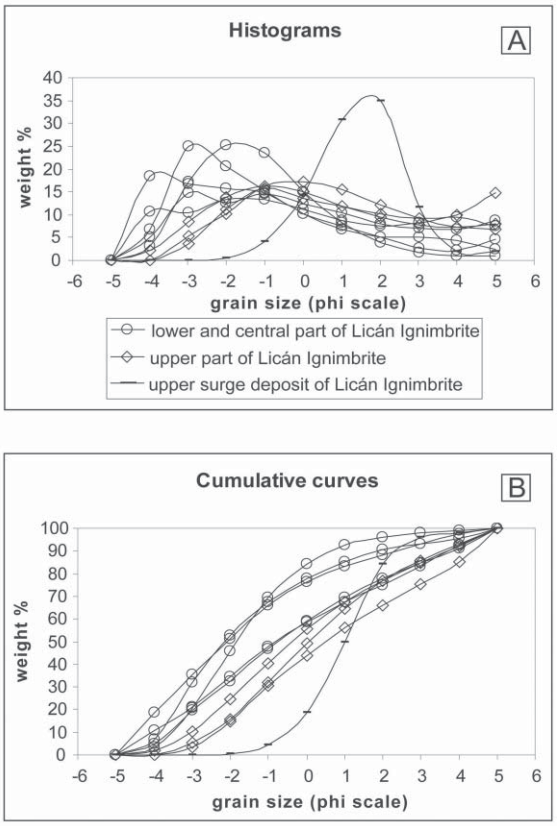

FIG. 5. Grain size analyses. **5A:** Histograms; **5B:** Cumulative curves (same symbols as in A). To limit the fragmentation of the material during sieving, the amplitude was regulated on 1.7 mm during 5 minutes.

LITHOLOGY

COMPONENTS

The 1 mm-fraction of the matrix from nine samples has been washed and counted by groups of 500 grains under binocular lenses. Five classes of fragments are recognized, three of them correspond to juvenile clasts; the other two are represented by free minerals and accidental lithic fragments (Table 1).

Class 1: are highly vesicular glassy juvenile grains, with irregular shapes. The grain morphology is characterised by the abundance and shape of the vesicles. A few grains show elongation of vesicles. Densities, measured on ten vesicular, lapilli-sized samples by determining weights in air and in water, range from 0.58 to 1.0 g/cm^3, confirming that mafic pumices (defined as juvenile material with density < 1 g/cm^3) are present in Licán deposits. The vesicularity index, calculated assuming a solid density of 2.59 g/cm^3 (andesitic composition; Hall, 1996) and using the method of Houghton and Wilson (1989), is comprised between 61 and 77%.

Class 2: are moderately vesicular juvenile grains. Grain morphology is independent of the shape of the vesicles. Regular shapes are sometimes bounded by more or less planar fractures.

Class 3: are non-vesicular or poorly vesicular grains. They are blocky, regular in shape with near planar faces forming 90°-angles between them.

Class 4: are fragments formed by single crystals, mainly of feldspars, sometimes covered with glass, and some honey coloured clinopyroxene crystals.

Class 5: are oxidized xenoliths of altered andesites and granitoids. Xenoliths of andesite are lighter-coloured than the juvenile material. Surfaces altered to manganese oxide are frequently observed.

VERTICAL VARIATIONS

The mean xenolith content of Licán deposits is high: 31% of grains (Table 1). Individual samples range from 16 to 60% (Table 1). The highest values (41 to 60%) are found at the summit of the sequences, presenting the upper surge deposit the maximum xenolith content (Table 1). Such a xenolith-enrichment towards the top is clearly seen at sites 5 and 54 (samples 5.1 and 54a, both at the top of sections *versus* samples 5.3 and 54b, both at the base, Table 1; Figs. 2 and 4). Vitreous ash is palagonitized in xenolith-rich samples and the upper parts of the deposits have generally a yellow, pale green or orange colour. To better consider the real proportions of juvenile ash types, percentages of classes 1 to 3 were recalculated without xenoliths and xenocrysts (Table 2). Xenolith enrichment in the upper levels is accompanied by a decrease in the proportion of highly vesicular grains and an increase in the class 3/class 1+2 ratio.

SURFACE TEXTURES

SEM images of Licán juvenile and accidental particles have been performed on the fine fraction (32 to 63 µm in size), separated without mechanical sieving. To preserve the original fragmentation, they were only washed with acetone and underwent 30 seconds in an ultrasound bath.

TABLE 1. LITHOLOGIC COUNTING RESULTS IN % OF GRAINS. SEE TEXT FOR EXPLANATION.

	Pyroclastic flow deposits									Surge deposit
Distance to the vent	~ 14 km W			~ 16 km NW	~ 16 km NNW	~ 22 km W		~ 35 km S		~ 27 km W
Position in the section	top	base	base	base	base	top	base	top		top
Sample No.	**54a**	**54b**	**55b**	**31**	**9**	**5.1**	**5.3**	**18**		**23.4**
									Mean	
Class 1 (highly vesicular juvenile grains)	19.0	38.4	37.0	28.0	17.4	2.8	19.2	24.8	23.3	10.2
Class 2 (moderately vesicular juvenile grains)	25.8	34.4	33.6	31.8	44.2	23.6	30.6	29.0	31.6	16.8
Class 3 (non-vesicular or poorly vesicular grains)	12.4	10.0	7.2	11.8	15.6	11.8	25.8	6.4	12.6	11.4
Class 4 (crystal fragments)	1.4	0.8	0.8	1.4	2.0	2.6	2.4	0.8	1.5	2.0
Class 5 (xenoliths)	41.4	16.4	21.4	27.0	20.8	59.2	22.0	39.0	30.9	59.6
Total	100	100	100	100	100	100	100	100	100	100

TABLE 2. LITHOLOGIC COUNTING RESULTS IN % OF GRAINS, RECALCULATED WITHOUT FREE MINERALS AND XENOLITHS.

	Pyroclastic flow deposits									Surge deposit
Distance to the vent	~ 14 km W			~ 16 km NW	~ 16 km NNW	~ 22 km W		~ 35 km S		~ 27 km W
Position in the section	top	base	base	base	base	top	base	top		top
Sample No.	**54a**	**54b**	**55b**	**31**	**9**	**5.1**	**5.3**	**18**		**23.4**
									Mean	
Class 1 (highly vesicular juvenile grains)	33.2	46.4	47.6	39.1	22.5	7.3	25.4	41.2	32.8	26.6
Class 2 (moderately vesicular juvenile grains)	45.1	41.5	43.2	44.4	57.3	61.8	40.5	48.2	47.7	43.8
Class 3 (non-vesicular or poorly vesicular grains)	21.7	12.1	9.3	16.5	20.2	30.9	34.1	10.6	19.4	29.7
Total	100	100	100	100	100	100	100	100	100	100

• The vesicular grains, equivalent to juvenile classes 1 and 2, are abundant with variable size of vesicles (most representative size: 0.01 mm). They have regular forms with plane or curved-planar fractures that cut the vesicles (Fig. 6A, B).

• Blocky, angular clasts (class 3; Fig. 6C) with no vesicles, occasionally exhibit stepped fractures (Fig. 6D).

• Aggregated grains. Adhesive particles are present on almost all grain surfaces, regardless of their morphology, but grains entirely formed by aggregated particles also occur (Fig. 6E). Secondary crystallization, of probably zeolites, is observed in cavities between the particles.

• Another type of grains has irregular shapes defined by vesicles. Curved-planar smooth surfaces corresponding to bubble walls (Fisher, 1963) give them either flat or angular shapes, or typical Y-shape (Fig. 6F).

QUANTITATIVE 3D ASH SURFACE ANALYSIS

Multiple images corresponding to different object planes were taken in order to overcome limited depth-of-field on conventional light microscope, with the aim to estimate the elevation surface and thus to obtain 3D reconstruction. Detailed sample preparation, image analysis procedures and algorithms for 3D reconstruction can be found in Ersoy *et al.* (2006 and in press). Here, we calculated seven roughness descriptors (Ra, Rq, Rsk, Rku, Rp, Rv, Rt), greylevel standard deviations (sGL) and fractal dimensions on reconstructed 3D surface images (depth-maps) of ash particles from two samples, 5.1 and 5.3, respectively from the top and bottom of the deposits at site 5 (Figs. 2 and 4).

The average roughness (Ra) and the root-mean-square roughness (Rq) are 'roughness amplitude descriptors', which give an average measurement of the surface height. 'Statistical descriptors' are skewness (Rsk) and kurtosis (Rku) of the amplitude distribution function (ADF) which give the probability of a profile of the surface having a certain height, z, at any position x. 'Extreme value descriptors' depend on isolated events, *e.g.* the maximum peak height (Rp), the maximum valley depth (Rv) and the maximum peak to valley height (Rt).

Furthermore, gradient analysis on images yielded polar plots giving the preferred orientations of the structures on volcanic ash surfaces (for detailed applications on volcanic ash, see Ersoy *et al.*, 2006). Different shape descriptors like the aspect ratio, compactness, roundness and form factor were calculated on the polar plots according to Russ (1999). All parameters were subjected to correlation analysis. Calculation of Pearson correlation coef-

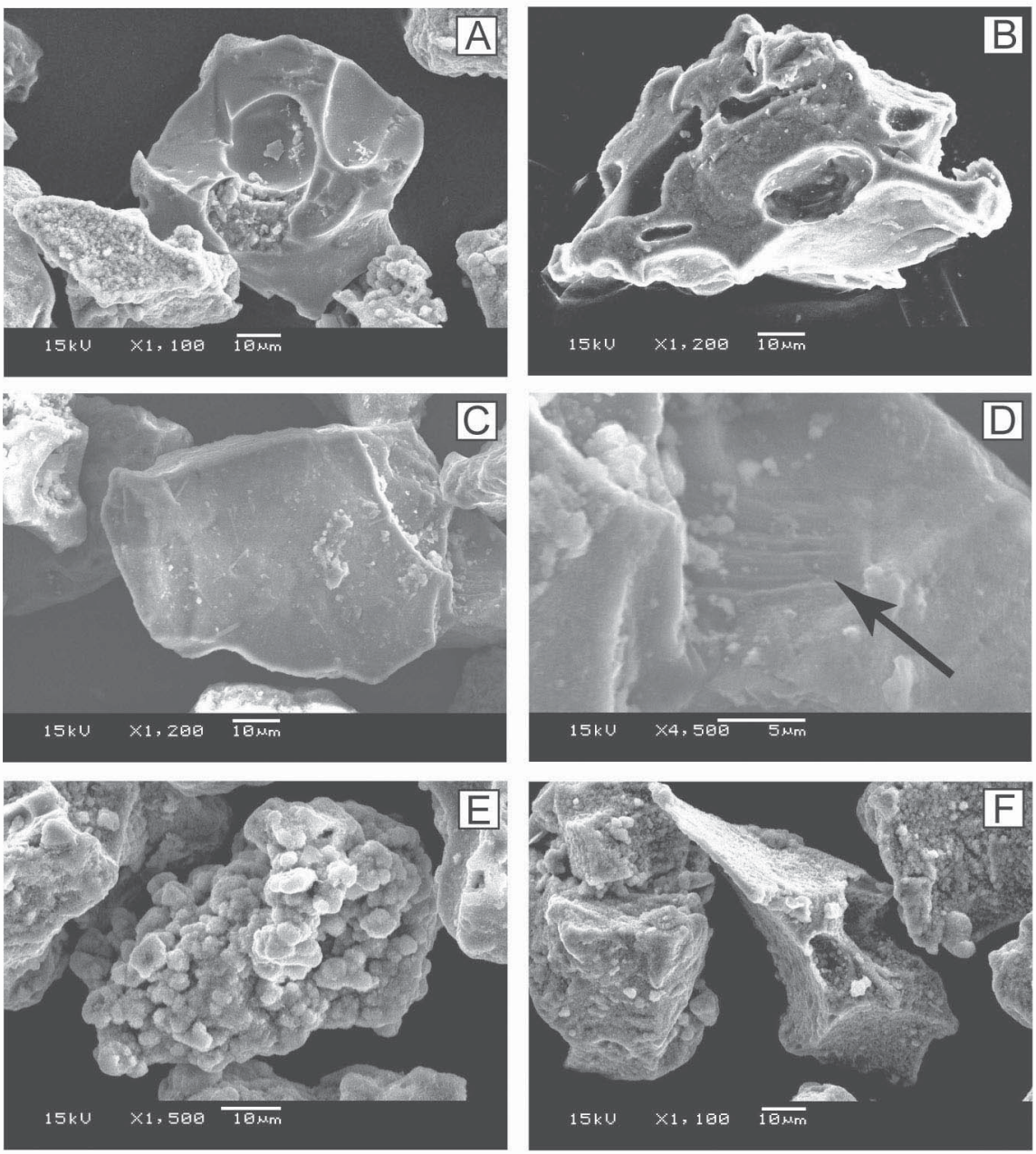

FIG. 6. SEM images of the Licán Ignimbrite, obtained with a JEOL-5910 scanning microscope operating at secondary electron mode with 15 keV, at Laboratoire Magmas et Volcans (Clermont-Ferrand, France).
Photos A and B: Vesicular regular grains with planar surfaces cutting the vesicles (scale 10 μm).
Photo C: Dense grain with surface of planar and stepped fractures (see photo D) (scale 10 μm).
Photo D: Detail of photo C showing the stepped fractures (arrow) (scale 5 μm).
Photo E: Aggregate of spherical particles (scale 10 μm).
Photo F: Bubble walls (scale 10 μm).

ficients was carried out in SPSS (SPSS Inc, Release 9.0). Pearson's correlation coefficient is a measure of linear association. We performed bivariate correlation procedures.

Fractal dimension (-0.92), the maximum valley depth (Rv) (-0.86) and skewness (Rsk) (0.80) are strongly correlated in each sample allowing discrimination between them (Fig. 7). Surface fractal dimension is between two for a smooth, regular surface and three for an infinitely porous medium. Thus, it is textural fractal dimension that represents surface irregularity/roughness and textural complexity (Huang *et al.*, 2001 and references therein). Although we expect lower complexity of the surfaces from sample 5.1 due to water interaction and limited vesiculation, they have higher fractal dimensions which were attributed to fine textures as a result of alteration and/or fine particle abundance on its surface. 'Extreme value descriptors' are also sensitive to adhering dust and alteration on surfaces. The 'statistical descriptor', Rsk, is sensitive to vesicles on ash surfaces and may be suitable for describing the vesicularity of the particles. Furthermore, 'statistical roughness descriptors' distinguish different pyroclast types, which results from different fragmentation mechanisms (Ersoy *et al.*, in press; Ersoy *et al.*, 2007).

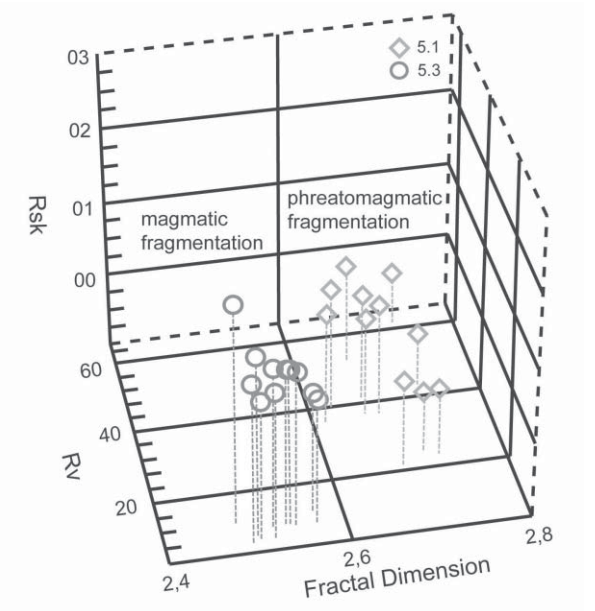

FIG. 7. 3D scatter plot of fractal dimension, Rsk (skewness) and Rv (maximum valley depth) values of surfaces from different types of volcanic ashes (samples 5.1 and 5.3; top and bottom of the Licán Ignimbrite, respectively).

SUMMARY OF PETROLOGY

Juvenile clasts from Licán Ignimbrite are generally sub-aphyric (only 3.5-6 vol% phenocrysts, recalculated to vesicle-free percentage) scoria and lapilli, with plagioclase (pl) as the main phenocryst-phase, followed by clinopyroxene (cpx), orthopyroxene (opx), olivine (ol) and titanomagnetite (Ti-mag). Groundmass is composed of pl, cpx, Ti-mag and variable amounts of glass (58-70% SiO_2), exhibiting intersertal or intergranular texture. Granitoid inclusions are common. Our ongoing mineralogical and textural studies are providing evidence that mixing is also an important petrological feature of the Licán Ignimbrite. As this is not the aim of this paper, only a brief summary will be given. Plagioclase phenocrysts belong to three compositional and textural groups: An_{74-91} (crystals with resorbed rims), An_{48-63} (euhedral-shaped crystals) and An_{35-44} (resorbed crystals). An-rich plagioclase is associated to Mg-rich olivine (Fo_{85}) which locally bears Cr-spinel inclusions. Euhedral-shaped plagioclase occurs with pyroxene of relatively high Mg number ($Mg\#_{cpx}$: 0.70-0.82; $Mg\#_{opx}$: 0.64-0.75) while sodic plagioclase is associated to Mg-poorer pyroxene ($Mg\#_{cpx}$: 0.57-0.68; $Mg\#_{opx}$: 0.47-0.59) ± apatite. Frequently, the less Mg-rich pyroxenes form resorbed cores, which are overgrown by Mg-rich rims (Fig. 8).

Twenty-six whole rock analyses have been carried out on juvenile material of the Licán deposits. They show a narrow silica content interval (55-58% SiO_2), similar to that reported in previous studies (Clavero, 1996), which clearly separates this series from overlying basaltic andesite Pucura lavas (53% SiO_2; Fig. 4). As a whole, volcanic rocks from Villarrica fit with the medium K calc-alkaline suites from continental arcs (Peccerillo and Taylor, 1976; Fig. 9A). On Harker diagrams (only MgO and Al_2O_3 are shown on Figs. 9B and C) a decreasing content in TiO_2, Al_2O_3, Fe_2O_3, MgO, CaO, Sc, V, Cr and Ni indicates that fractionation of olivine, pyroxene, plagioclase and Fe-Ti oxides is the major process responsible for the evolution of this magmatic suite, as has been suggested by previous studies (*e.g.,* Hickey-Vargas *et al.*, 2004).

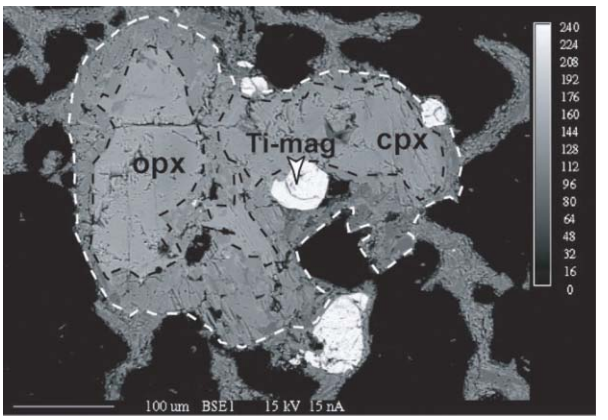

FIG. 8. Backscattered electron image of Licán Ignimbrite juvenile material. Resorbed cores of Mg-poor pyroxenes (limited by black stippled lines) overgrown by Mg-rich mantles (limited by white stippled lines). **Opx:** orthopyroxene; **cpx:** clinopyroxene; **Ti-mag:** titanomagnetite.

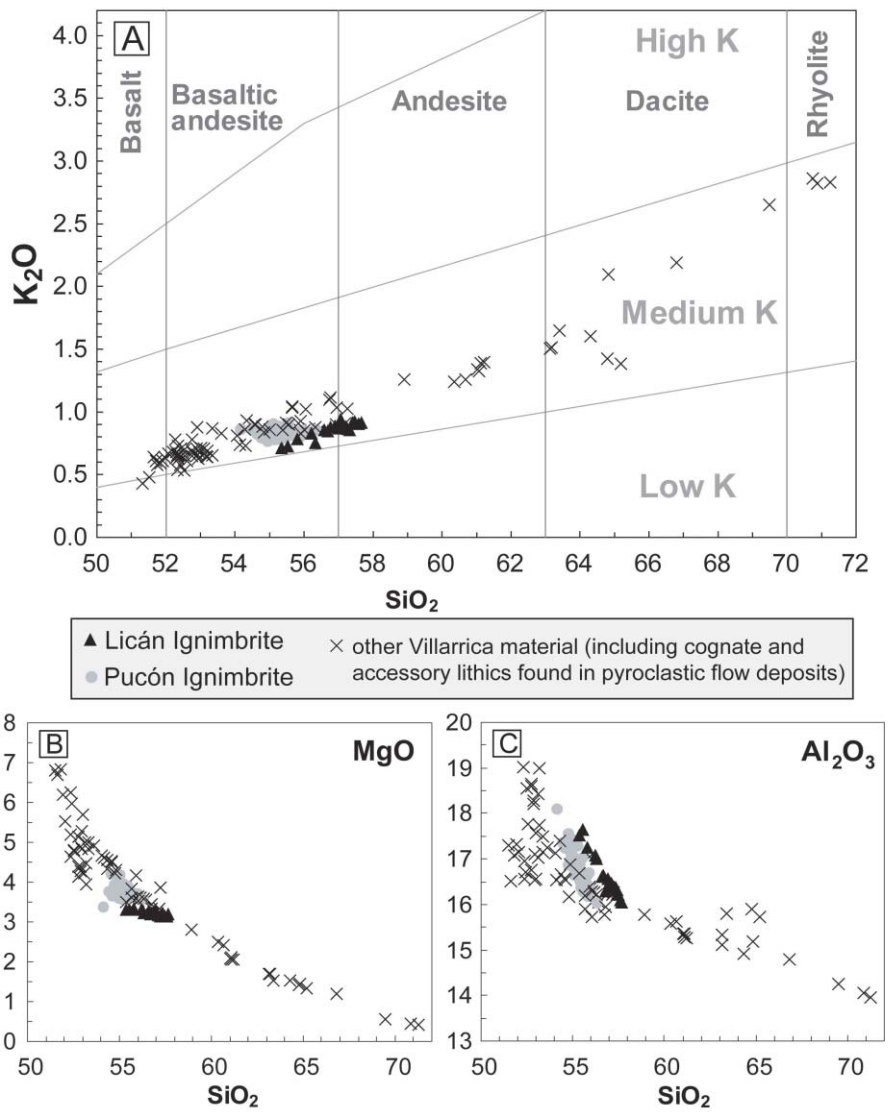

FIG. 9. Selected major element variations as a function of silica content (values in weight %). Limits in A according to Peccerillo and Taylor (1976).

DISCUSSION: INFLUENCE OF WATER DURING THE ERUPTION

In andesitic volcanoes, mafic pyroclastic flows generally involve small volumes of magma in the course of volcanic and magmatic cycles associated with periodic supply to the chamber (*e.g.,* Robin *et al.*, 1991). Large volume pyroclastic flow deposits of basaltic or basaltic andesite composition are scarce. However, few published studies document large magnitude pyroclastic eruptions involving mafic pyroclastic deposits. For example, Masaya volcano in Nicaragua generated a basaltic ignimbrite (8 km^3) during a caldera-forming eruption 2,500 years ago (Williams, 1983). At Tanna, Ambrym and Santa María (Vanuatu, New Hebrides arc), basaltic ash flows are related to eruptions which led to caldera collapse (Robin *et al.*, 1993, 1995). In Italy, De Rita *et al.* (2002) described large volume mafic ignimbrites of Middle Pleistocene age at Colli Albani volcano. In all these eruptions implying large volumes of mafic pyroclastic flows, the crucial role of phreatomagmatism has been either demonstrated or suggested. In Chile, in addition to Villarrica, Llaima volcano has experienced such large magnitude explosive eruptions related to basaltic andesite magma (Naranjo and Moreno, 1991).

Vesiculation indices as high as 77% show that at least part of the Licán magma was vesiculating to a point where it could have fragmented simply by bursting of bubbles (magmatic fragmentation is predicted at vesicle volumes of the order of 75-83%; Sparks, 1978). Many arc basalts have relatively high H_2O contents (2-6 wt%), as shown by experimental (*e.g.*, Sisson and Grove, 1993; Pichavant *et al.*, 2002) and phenocryst-hosted melt inclusion-studies (*e.g.*, Cervantes and Wallace, 2003; Gurenko *et al.*, 2005). Furthermore, the crystallization of anhydrous minerals (like pl, cpx, opx, ol, Ti-mag) produces volatile enrichment in the coexisting melt, provided that the pressure is high enough for the volatiles to remain in solution (*e.g.*, Burnham, 1979). This means that there would be no need of additional volatile enrichment to explain explosive basaltic volcanism. At Villarrica, however, Lohmar *et al.* (2006) pointed out that assimilation of hydrated and volatile-rich phases from basement plutonic rocks could additionally enrich the magma in volatiles, a hypothesis proposed by McCurry and Schmidt (2001) to explain the origin of Pucón Ignimbrite from Villarrica volcano. Additionally, our ongoing mineralogical studies show evidence for mixing in the Licán magma chamber. However, in this paper, field studies, together with grain size analyses, lithological counting and surface texture observations indicate that the high explosivity degree could be essentially due to (1) the presence of a high content of magmatic gas (whatever its origin, mantellic or crustal) and (2) phreatomagmatism. Below, we try to specify the role of this second process.

Phreatomagmatism is clearly supported by SEM images. Vesicles cut by plane or curved-planar fractures in ashes from class 2 (Fig. 6A,B) demonstrate that vesiculation was not the only process responsible for the fragmentation of the material. Moreover, dense vitreous clasts and the presence of stepped fractures observed on some grains (Fig. 6C, D) further indicate that these particles clearly result from a brittle process, that is, the deformation rate acting on the magma was so high, that liquid relaxation of the stresses could not occur (Büttner *et al.*, 1999). This fragile fracturation process can be related to the 'Molten Fuel Coolant Interaction' (MFCI) phenomenon (Wohletz, 1983; Zimanowski *et al.*, 1997a, b; Zimanowski, 1998). MFCI explosions result from the interaction of a hot fluid (fuel) with a cold fluid (coolant) whose vaporization temperature is below that of the former. The source of explosive energy is the rapid heat transfer from the melt to the water which produces explosive vaporization and abundant fine-grained debris (Wohletz, 1983). Such features (plane or curved-planar fractures that cut the vesicles, dense vitreous clasts, stepped fractures) occur mostly towards the top of the Licán deposits sequence, indicating that magma-water interaction increased drastically during the course of the eruption. Other morphological characteristics, such as adhesive and aggregated particles, have also been attributed to magma-water interactions (Heiken and Wohletz, 1985). The resulting particles (fragments of bubble walls, fragments of glass, lithics and spheric particles) form irregular grains of moss-like aspect (Fig. 6E). Secondary crystallization observed in certain blisters is also interpreted as being specific of this type of dynamism (Cioni *et al.*, 1992).

The 3D analysis of ash surfaces shows that the two kinds of fragmentation mechanisms, magmatic and phreatomagmatic, can be distinguished. Once again, the upper Licán deposits show a greater influence of phreatomagmatic process than the former ones (samples 5.1 and 5.3, respectively from the top and bottom of the Licán deposits; Fig. 7).

Summit horizons of Licán Ignimbrite (including surge deposits) are enriched in xenoliths and show a lower grain-size mean, compared to the base of the deposit (Table 1; Fig. 5B). This indicates a higher degree of fragmentation which can also be explained by phreatomagmatism. Xenolith enrichment in the upper levels is accompanied by a decrease in the proportion of highly vesicular grains and an increase in non-vesicular or poorly vesicular grains, indicating a decrease of the influence of magmatic fragmentation with time during the eruption. Experimentally, it was established that the strongest degree of explosiveness is obtained for a water-magma ratio between 0.3 and 0.4 (Wohletz and McQueen, 1984). Above and below these values, the explosiveness decreases quickly. The xenolith-rich samples from the upper part of the deposits suggest a greater contribution from the conduit, mainly by mechanical abrasion. Thus, lithologic characteristics suggest an increase in the amount of water supply in the conduit, possibly in relation with vent enlargement and caldera formation. Conversely, magmatic fragmentation decreased. The pattern of increasing phreatomagmatism with time, presented here for Licán Ignimbrite, has been described elsewhere and was first developed by Sheridan *et al.* (1981) for Vesuvius volcano (Italy).

CONCLUSION

Licán pyroclastic deposits represent a major explosive eruption of Villarrica volcano that occurred in the Late Glacial Period, about 13,800 years BP. The Licán eruption seems to have been a single event producing juvenile material with a moderate degree of differentiation (55-58% SiO_2).

Magma-water interaction was a key factor in the Licán Ignimbrite-eruption which can explain its increasing explosive behaviour. The eruptive dynamics is characterised by the coexistence of two types of fragmentation: (1) a magmatic one, which correspond to vesiculation and gas expansion and (2) a phreatomagmatic one due to magma-water interaction. The latter is clearly evidenced by the 3D quantitative analysis of ash surface and textural observations: more or less vesicular ash showing faces that cut the vesicles, blocky shaped ashes with stepped fractures and adhesive and aggregated particles, all features that underline a brittle and intense fragmentation related to water-magma interaction. These characteristics are rather specific of the upper part of the Licán deposits sequence. Conversely, the occurrence of vesiculated clasts, including mafic pumices, is more abundant at the base of the Licán ignimbritic sequence. This, together with the high xenolith content in the upper part of deposits, the grain-size data and lithological countings, emphasizes the increasing role of phreatomagmatic fragmentation during the evolution of the eruptive cycle.

ACKNOWLEDGEMENTS

This research was funded through the collaborative ECOS-CONICYT Project No. C01U03 involving IRD (Institut de Recherche pour le Développement, France), GEA (Instituto de Geología Económica Aplicada, Universidad de Concepción, Chile), SERNAGEOMIN (Servicio Nacional de Geología y Minería, Chile) and Universidad de Chile (Santiago de Chile). Funding has also been provided by the Institut de Recherche pour le Développement (UR 31 'Processus et Aléas Volcaniques' and M163 'Magmas et Volcans'). Julien Vennat is gratefully acknowledged for doing SEM and lithological analyses. SL acknowledges the support given by a MECESUP grant.

The authors are grateful for constructive remarks and English corrections by A. Demant (Université Paul Cézanne, Aix-Marseille 3, France), S. Sparks (University of Bristol, United Kingdom) and B. Zimanowski (Universität Würzburg, Germany) which significantly improved the manuscript. The editor of the Revista Geológica de Chile (M. Suárez) is also acknowledged for helpful comments.

REFERENCES

Burnham, C.W. 1979. The importance of volatile constituents. *In* The evolution of igneous rocks: Fiftieth Anniversary Perspectives (Joder, H.S. Jr.; editor). Princeton University Press*:* 439-482.

Büttner, R.; Dellino, P.; Zimanowski, B. 1999. Identifying magma-water interaction from the surface features of ash particles. Nature 401: 688-690.

Cembrano, J.; Hervé, F.; Lavenu, A. 1996. The Liquiñe-Ofqui fault zone: a long-lived intra-arc fault system in southern Chile. Tectonophysics 259: 55-66.

Cervantes, P.; Wallace, P.J. 2003. Role of H_2O in subduction-zone magmatism: new insights from melt inclusions in high-Mg basalts from central Mexico. Geology 31: 235-238.

Cioni, R.; Sbrana, A.; Vecci, R. 1992. Morphologic features of juvenile pyroclasts from magmatic and phreatomagmatic deposits of Vesuvius. Journal of Volcanology and Geothermal Research 51 (1-2): 61-78.

Clapperton, C. 1993. Quaternary geology and geomorphology of South America. Elsevier Science Publishers: 779 p.

Clavero, J. 1996. Ignimbritas andesítico-basálticas postglaciales del Volcán Villarrica, Andes del Sur (39°25'S). Tesis de Magíster (Unpublished), Universidad de Chile, Departamento de Geología: 112 p.

Clavero, J.; Moreno, H. 1994. Ignimbritas Licán y Pucón: Evidencias de erupciones explosivas andesítico-basálticas postglaciales del Volcán Villarrica, Andes del Sur, 39°25'S. *In* Congreso Geológico Chileno, No. 7, Actas 1: 250-254. Concepción.

Clavero, J.; Moreno, H. 2004. Evolution of Villarrica Volcano. *In* Villarrica Volcano (39.5°S), Southern Andes, Chile (Lara, L.; Clavero, J.; editors). Servicio Nacional de Geología y Minería, Boletín 61: 17-27.

Denton, G.H.; Heusser, C.J.; Lowell, T.V.; Moreno, P.I.; Andersen, B.G.; Heusser, L.E.; Schlüchter, C.; Marchant, D.R. 1999. Interhemispheric linkage of paleoclimate during the last glaciation. Geografiska Annaler 81A (2): 107-153.

De Rita, D.; Giordano, G.; Esposito, A.; Fabbri, M.; Rodani, S. 2002. Large volume phreatomagmatic ignimbrites from the Colli Albani volcano (Middle Pleistocene, Italy). Journal of Volcanology and Geothermal Research 118: 77-98.

Ersoy, O.; Chinga, G.; Aydar, E.; Gourgaud, A.; Cubukcu, H.E.; Ulusoy, I. 2006. Texture discrimination of volcanic ashes from different fragmentation mechanisms: A case study, Mount Nemrut stratovolcano, eastern Turkey. Computers and Geosciences 32 (7): 936-946.

Ersoy, O.; Aydar, E.; Gourgaud, A.; Bayhan, H. In press. Quantitative analysis on volcanic ash surfaces: Application of extended depth-of-field (focus) algorithm for light and scanning electron microscopy and 3D reconstruction. Micron.

Ersoy, O.; Gourgaud, A.; Aydar, E.; Chinga, G.; Thouret, J.-C. 2007. Quantitative SEM analysis of volcanic ash surfaces: application to the 1982-83 Galunggung eruption (Indonesia). Geological Society of America Bulletin 119 (5): 743-752.

Fisher, R.V. 1963. Bubble-wall texture and its significance. Journal of Sedimentary Petrology 33: 224-227.

Fisher, R.V.; Schmincke, H.U. 1984. Pyroclastic Rocks. Springer Verlag: 472 p.

Gaytán, D.; Clavero, J.; Rivera, A. 2005. Actividad eruptiva explosiva del Volcán Villarrica, Andes del Sur (39.5°S), durante la glaciación Llanquihue. *In* Congreso Geológico Argentino, No. 16, CD-ROM. La Plata.

González-Ferrán, O. 1995. Volcanes de Chile. Instituto Geográfico Militar: 640 p.

Gurenko, A.A.; Belousov, A.B.; Trumbull, R.B.; Sobolev, A.V. 2005. Explosive basaltic volcanism of the Chikurachki Volcano (Kurile arc, Russia): Insights on pre-eruptive magmatic conditions and volatile budget revealed from phenocryst-hosted melt inclusions and groundmass glasses. Journal of Volcanology and Geothermal Research 147: 203-232.

Hall, A. 1996. Igneous Petrology, 2nd Edition. Longman Group Limited: 551 p.

Heiken, G.; Wohletz, K. 1985. Volcanic ash. University of California press: 246 p.

Herron, E.M.; Cande, S.C.; Hall, B.R. 1981. An active spreading center collides with a subduction zone: A geophysical survey of the Chile Margin triple junction. Geological Society of America, Memoir 154: 683-701.

Hickey-Vargas, R.; López-Escobar, L.; Moreno, H.; Clavero, J.; Lara, L.; Sun, M. 2004. Magmatic evolution of the Villarrica Volcano. *In* Villarrica Volcano (39.5°S), Southern Andes, Chile (Lara, L.; Clavero, J.; editors). Servicio Nacional de Geología y Minería, Boletín 61: 39-45.

Houghton, B.F.; Wilson, C.J.N. 1989. A vesicularity index for pyroclastic deposits. Bulletin of Volcanology 51: 451-462.

Huang, W.L.; Shi, H.C.; Kai, M.L.; Shou, R.G. 2001. Influence of calcining temperature on the mesopore structures and surface fractal dimensions of MgO-Al_2O_3-SiO_2 xerogels. Journal of Physics and Chemistry of Solids 62 (7): 1205-1211.

Lara, L. 2004. Villarrica-Lanín chain: Tectonic constraints for volcanism in a transversal alignment. *In* Villarrica Volcano (39.5°S), Southern Andes, Chile (Lara, L.; Clavero, J.; editors). Servicio Nacional de Geología y Minería, Boletín 61: 13-16.

Lohmar, S.; Parada, M.A.; Robin, C.; Gerbe, M.C.; Deniel, C.; Gourgaud, A; López-Escobar, L.; Moreno, H.; Naranjo, J.A. 2006. Origin of postglacial 'mafic' ignimbrites at Llaima and Villarrica volcanoes (Southern Andes, Chile): Assimilation of plutonic rocks as one of the triggering factors? *In* Simposio Sudamericano de Geología Isotópica (SSAGI), No. 5, CD-ROM. Punta del Este.

López-Escobar, L.; Cembrano, J.; Moreno, H. 1995. Geochemistry and tectonics of the Chilean Southern Andes basaltic Quaternary volcanism (37-46°S). Revista Geológica de Chile 22 (2): 219-234.

Lowell, T.V.; Heusser, C.J.; Andersen, B.G.; Moreno, P.I.; Hauser, A.; Heusser, L.E.; Schlüchter, C.; Marchant, D.R.; Denton, G.H. 1995. Interhemispheric correlation of Late Pleistocene glacial events. Science 269: 1541-1549.

McCulloch, R.D.; Bentley, M.J.; Purves, R.S.; Hulton, N.R.J.; Sugden, D.E.; Clapperton, C.M. 2000. Climatic inferences from glacial and palaeoecological evidence at the last glacial termination, southern South America. Journal of Quaternary Science 15 (4): 409-417.

McCurry, M.; Schmidt, K. 2001. Petrology and Oxygen Isotope Geochemistry of the Pucón Ignimbrite-Southern Andean Volcanic Zone, Chile: Implications for Genesis of Mafic Ignimbrites. *In* Simposio Sudamericano de Geología Isotópica (SSAGI), No. 3, CD-ROM. Pucón.

Moreno, H.; Clavero, J. 2006. Geología del área del Volcán Villarrica. Servicio Nacional de Geología y Minería, Serie Geología Básica, Carta Geológica de Chile, No. 98, escala 1:50.000.

Naranjo, J.A.; Moreno, H. 1991. Actividad explosiva postglacial en el Volcán Llaima, Andes del Sur (38°45'S). Revista Geológica de Chile 18 (1): 69-80.

Peccerillo, R.; Taylor, S.R. 1976. Geochemistry of Eocene calc-alkaline volcanic rocks from the Kastamonu area, northern Turkey. Contributions to Mineralogy and Petrology 58: 63-81.

Petit-Breuilh, M.E.; Lobato, J. 1994. Análisis comparativo de la cronología eruptiva histórica de los volcanes Llaima y Villarrica (38°-39° L.S.). *In* Congreso Geológico Chileno, No. 7, Actas 1: 366-370. Concepción.

Pichavant, M.; Mysen, B.O.; Macdonald, R. 2002. Source and H_2O content of high-Mg magmas in island arc settings: an experimental study of a primitive calc-alkaline basalt from St. Vicent, Lesser Antilles arc. Geochimica et Cosmochimica Acta 66: 2193-2209.

Robin, C.; Camus, G.; Gourgaud, A. 1991. Eruptive and magmatic cycles at Fuego de Colima volcano (Mexico). Journal of Volcanology and Geothermal Research 45: 209-225.

Robin, C.; Eissen, J.P.; Monzier, M. 1993. Giant tuff cone and 12 km-wide associated caldera at Ambrym (New Hebrides Arc). Journal of Volcanology and Geothermal Research 55: 225-238.

Robin, C.; Eissen, J.P.; Monzier, M. 1995. Mafic pyroclastic flows at Santa María (Gaua) Volcano, Vanuatu: The caldera formation problem in mainly mafic island arc volcanoes. Terra Nova 7 (4): 436-443.

Russ, J.C. 1999. The image processing handbook. Third edition, CRC Press: 771 p.

Sheridan, M.F.; Barberi, F.; Rosi, M.; Santacroce, R. 1981. A model for Plinian eruptions of Vesuvius. Nature 289: 282-285.

Silva, C.; Druitt, T.; Robin, C.; Lohmar, S.; Clavero, J.; Moreno, H.; Naranjo, J.A. 2004. The 3700-yr Pucón eruption of Villarrica volcano, 39°S Southern Andes, Chile. *In* International Association of Volcanology and Chemistry of the Earth's Interior (IAVCEI), CD-ROM. Pucón.

Sisson, T.W.; Grove, T.L. 1993. Experimental investigations of the role of H_2O in calc-alkaline differentiation and subduction zone magmatism. Contributions to Mineralogy and Petrology 113: 143-166.

Sparks, R.S.J. 1978. The dynamics of bubble formation and growth in magmas: a review and analysis. Journal of Volcanology and Geothermal Research 3: 1-37.

Walker, G.P.L. 1971. Grain-size characteristics of pyroclastic deposits. Journal of Geology 79: 696-714.

Williams, S. 1983. Geology and eruptive mechanisms of Masaya caldera complex, Nicaragua. Ph.D. Thesis (Unpublished), Darthmonth College Hanover: 169 p.

Wohletz, K.H. 1983. Mechanisms of hydrovolcanic pyroclasts formation: grain size, scanning electron microscopy, and experiments studies. Journal of Volcanology and Geothermal Research 17: 31-64.

Wohletz, K.H.; McQueen, R.G. 1984. Volcanic and stratospheric dustlike particles produced by experimental water-melt interactions. Geology 12: 591-594.

Zimanowski, B. 1998. Phreatomagmatic explosions. *In* From magma to tephra (Freundt, A.; Rosi, M.; editors). Elsevier: 25-54.

Zimanowski, B.; Büttner, R.; Lorentz, V. 1997a. Premixing of magma and water in MFCI experiments. Bulletin of Volcanology 58: 491-495.

Zimanowski, B.; Büttner, R.; Lorenz, V.; Häfele, H.G. 1997b. Fragmentation of basaltic melt in the course of explosive volcanism. Journal of Geophysical Research 102: 803-814.

Manuscript received: September 6, 2006; accepted: April 10, 2007.